be explained by the indirect aerosol cloud effect. The use of a parcel model to determine the cloud droplet number concentration enables us to separate the effects of the cloud LWP and cloud droplet number concentration on the cloud optical depth. An examination of the TOA shortwave flux from the radiative transfer model applied to the two sites does not directly confirm the indirect effect, because the observed surface albedos at the NSA site for our cases (0.6 ± 0.28) are significantly larger than those from the SGP site (0.2 ± 0.02). However, the model can be used to estimate the outgoing flux difference if the clouds from the NSA site had the same average surface albedo and average zenith angle as those from the SGP site (see Fig. 3). This analysis indicates that these sites provide important evidence corroborating the effect of aerosols on cloud optical properties and on shortwave fluxes at both the surface and the TOA. Moreover, the analysis indicates that a parameterization of the effects of aerosols on clouds on the basis of an adiabatic parcel model and average aerosol size distributions such as those used in current general circulation models[18,22,23] provides a good estimate of cloud optical properties determined over a broad range of aerosol concentrations. □

Received 28 May; accepted 17 November 2003; doi:10.1038/nature02234.

1. Penner, J. E. *et al.* in *Climate Change 2001: The Scientific Basis* (eds Houghton, J. T. *et al.*) 289–348 (Cambridge Univ. Press, Cambridge, UK, 2001).
2. Rosenfeld, D. & Feingold, G. Explanation of discrepancies among satellite observations of the aerosol indirect effects. *Geophys. Res. Lett.* **30,** doi:10.1029/2003GL017684 (2003).
3. Brenguier, J.-L., Pawlowska, H. & Schüller, L. J. Cloud microphysical and radiative properties for parameterization and satellite monitoring of the indirect effect of aerosol on climate. *J. Geophys. Res.* **108,** doi:101029/2002JD002682 (2003).
4. Sheridan, P. J., Delene, D. J. & Ogren, J. A. Four years of continuous surface aerosol measurements from the Department of Energy's Atmospheric Radiation measurement Program Southern Great Plains Cloud and Radiation Testbed site. *J. Geophys. Res.* **106,** 20735–20747 (2001).
5. Dong, X., Ackerman, T. P., Clothiaux, E. E., Pilewskie, P. & Han, Y. Microphysical and radiative properties of stratiform clouds deduced from ground-based measurements. *J. Geophys. Res.* **102,** 23829–23843 (1997).
6. Dong, X., Ackerman, T. P. & Clothiaux, E. E. Parameterizations of microphysical and shortwave radiative properties of boundary layer stratus from ground-based measurements. *J. Geophys. Res.* **102,** 31681–31393 (1998).
7. Dong, X., Mace, G. G., Minnis, P. & Young, D. F. Arctic stratus cloud properties and their effect on the surface radiation budget: selected cases from FIRE ACE. *J. Geophys. Res.* **106,** 15297–15312 (2001).
8. Dong, X. *et al.* Comparison of stratus cloud properties deduced from surface, GOES, and aircraft data during the March 2000 ARM Cloud IOP. *J. Atmos. Sci.* **59,** 3265–3284 (2002).
9. Dong, X. & Mace, G. G. Profiles of low-level stratus cloud microphysics deduced from ground-based measurements. *J. Atmos. Ocean. Tech.* **20,** 42–53 (2003).
10. Liljegren, J. C., Clothiaux, E. E., Mace, G. G., Kato, S. & Dong, X. A new retrieval for liquid water path using a ground based microwave radiometer and measurements of cloud temperature. *J. Geophys. Res.* **106,** 14485–14500 (2001).
11. Dong, X. & Mace, G. G. Arctic stratus cloud properties and radiative forcing derived from ground-based data collected at Barrow Alaska. *J. Clim.* **16,** 445–461 (2003).
12. Liu, X. & Seidl, W. Modeling study of cloud droplet nucleation and in-cloud sulfate production during the Sanitation of the Atmosphere (SANA) 2 campaign. *J. Geophys. Res.* **103,** 16145–16158 (1998).
13. Delene, D. J. & Deshler, T. Vertical profiles of cloud condensation nuclei above Wyoming. *J. Geophys. Res.* **106,** 12579–12588 (2001).
14. Quinn, P. K. *et al.* A three-year record of simultaneously measured aerosol chemical and optical properties at Barrow, Alaska. *J. Geophys. Res. D* **107,** doi:101029/2001JD001248 (2002).
15. Climate Modeling and Diagnostics Laboratory data archive ⟨http://www.cmdl.noaa.gov/info/ftpdata.html⟩ (2000).
16. Twomey, S. The nuclei of natural clouds formation. Part II: The supersaturation in natural clouds and the variation of cloud droplet concentration. *Geofis. Pura Appl.* **43,** 243–249 (1959).
17. Rogers, E., Deaven, D. G. & DiMego, G. J. The regional analysis system for the operational "early" eta model: original 80-km configuration and recent changes. *Weath. Forecast.* **10,** 810–825 (1995).
18. Lohmann, U., Feichter, J., Chuang, C. C. & Penner, J. E. Prediction of the number of cloud droplets in the ECHAM GCM. *J. Geophys. Res.* **104,** 9169–9198 (1999).
19. Brenguier, J.-L. *et al.* Radiative properties of boundary layer clouds: droplet effective radius versus number concentration. *J. Atmos. Sci.* **57,** 803–821 (2000).
20. Liu, Y. & Daum, P. H. Indirect warming effect from dispersion forcing. *Nature* **419,** 580–581 (2002).
21. Lin, B., Wielicki, B., Minnis, P. & Rossow, W. Estimation of water cloud properties from satellite microwave, infrared, and visible measurements in oceanic environments. 1, Microwave brightness temperature simulations. *J. Geophys. Res.* **103,** 3873–3886 (1998).
22. Ghan, S. J., Easter, R. C., Hudson, J. & Breon, F.-M. Evaluation of aerosol indirect radiative forcing in MIRAGE. *J. Geophys. Res.* **106,** 5317–5334 (2001).
23. Chuang, C. C. *et al.* Cloud susceptibility and the first aerosol indirect forcing: Sensitivity to black carbon and aerosol concentrations. *J. Geophys. Res. D* **107,** doi:101029/2000JD000215 (2002).

Acknowledgements We thank P. Quinn for providing the composition data at the ARM SGP and NSA sites. During this study, X.D. was also supported by the NASA CERES project. This work was supported by the DOE ARM programme.

Competing interests statement The authors declare that they have no competing financial interests.

Correspondence and requests for materials should be addressed to J.E.P. (penner@umich.edu).

Tungsten isotope evidence that mantle plumes contain no contribution from the Earth's core

Anders Scherstén[1], Tim Elliott[1], Chris Hawkesworth[1] & Marc Norman[2]

[1]*Department of Earth Sciences, University of Bristol, Will's Memorial Building, Queen's Road, Bristol BS8 1RJ, UK*
[2]*Research School of Earth Sciences, The Australian National University, Canberra, Australian Capital Territory 0200, Australia*

Osmium isotope ratios provide important constraints on the sources of ocean-island basalts, but two very different models have been put forward to explain such data. One model interprets ^{187}Os-enrichments in terms of a component of recycled oceanic crust within the source material[1,2]. The other model infers that interaction of the mantle with the Earth's outer core produces the isotope anomalies and, as a result of coupled ^{186}Os–^{187}Os anomalies, put time constraints on inner-core formation[3–5]. Like osmium, tungsten is a siderophile ('iron-loving') element that preferentially partitioned into the Earth's core during core formation but is also 'incompatible' during mantle melting (it preferentially enters the melt phase), which makes it further depleted in the mantle. Tungsten should therefore be a sensitive tracer of core contributions in the source of mantle melts. Here we present high-precision tungsten isotope data from the same set of Hawaiian rocks used to establish the previously interpreted ^{186}Os–^{187}Os anomalies and on selected South African rocks, which have also been proposed to contain a core contribution[6]. None of the samples that we have analysed have a negative tungsten isotope value, as predicted from the core-contribution model. This rules out a simple core–mantle mixing scenario and suggests that the radiogenic osmium in ocean-island basalts can better be explained by the source of such basalts containing a component of recycled crust.

Many ocean-island basalts are thought to be the surface expression of mantle plumes that originate from a boundary layer within the mantle. Ocean-island basalts are geochemically distinct from mid-ocean-ridge basalts, and the differences are often attributed to recycled components of crust or ancient melt-depleted lithosphere[7,8]. It has been argued that the Re–Os system provides powerful evidence for recycled components because Re/Os ratios are high in melts and correspondingly low in residues, which with time develop increasingly radiogenic and depleted Os-isotope compositions respectively[1,2,9,10]. Yet Re–Os is also fractionated by inner-core crystallization, where Os partitions into the inner core leaving the outer core with a high Re/Os ratio. Thus, small core contributions are an alternative explanation for the occurrence of radiogenic Os in ocean-island basalts[11].

In principle, such core contributions can be tested using combined ^{186}Os–^{187}Os isotopes, because Pt–Os fractionates in the same way as Re–Os during inner-core crystallization and ^{190}Pt decays to ^{186}Os. In view of the long half-lives of ^{190}Pt ($T_{1/2} \approx 450$ Gyr) and

^{187}Re ($T_{1/2} \approx 42$ Gyr), Pt–Os and Re–Os fractionation would need to have taken place early in Earth's history to produce significant anomalies in the Os isotope system. Coupled ^{186}Os–^{187}Os anomalies for Hawaiian picrites and Gorgonan komatiites have been attributed to small core contributions[3–5]. If correct, this puts major constraints on the origins of such plumes and core evolution: (1) providing geochemical evidence for mantle plumes originating at the core–mantle boundary, and (2) requiring inner-core crystallization start early at 3.5 Gyr ago or earlier[5]. Independently verifying the presence of core material in the source of ocean-island basalt thus has great significance.

A new test for core interaction is now available from W isotopes and the extinct ^{182}Hf–^{182}W system. Hf and W are both refractory elements, but because Hf is lithophile it will remain in the silicate Earth whereas the siderophile W will preferentially partition into the metallic core. Hence the silicate Earth is highly depleted in W with respect to C1 chondrite. This can be expressed in terms of the ratio of W to a refractory lithophile element of similar incompatibility (such as Th; ref. 12); C1 chondrite has W/Th $\approx$ 3.2, whereas silicate Earth has W/Th$_{sE}$ between 0.14–0.26, with a best estimate of 0.19 (ref. 12). ^{182}Hf ($T_{1/2} \approx 9$ Myr) was extant at the formation of the Solar System (t_0) and recent data show that chondritic W-isotope ratios are two epsilon units (ϵW, see Fig. 1 for definition) lower than silicate Earth[13–15] (Table 1), which is zero by definition. This implies that Earth's core formation occurred ~10–30 Myr after t_0 depending on whether a continuous or a simple two-stage differentiation model is assumed[13]. Regardless of the timing or style of core formation, mass balance requires the core to have a $\epsilon W = -2.1$ if bulk Earth is assumed to be chondritic and silicate Earth W/Th$_{sE}$ = 0.19. This value varies by only ~0.1 ϵW for residual silicate Earth W/Th ratios in the range 0.14–0.26. Thus, the W-isotope budget of the Earth is well established. Critically, differences in W isotopes are imparted only at the beginning of Earth history and further differentiation processes do not affect them. This is not true for the long-lived Pt–Os and Re–Os systems, as parent–daughter fractionation at any time in Earth history will yield variable present-day Os isotopic anomalies depending on time, degree of fractionation and parent half-life. Taken together, these features make W isotopes particularly powerful as an independent test of the core-contribution model.

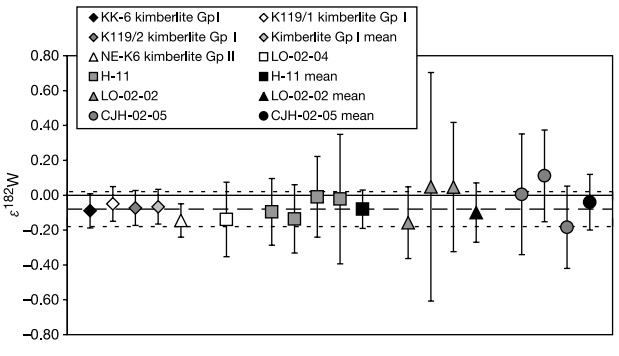

Figure 1 ϵW values for Group I and Group II kimberlites and Hawaiian picrites. ϵW was calculated using the average for the NIST SRM3163 standard solution for each analytical session: $\epsilon W = ([^{182}W/^{184}W]spl/[^{182}W/^{184}W]SRM3163–1) \times 10{,}000$. To ensure that anomalies were not introduced by our chemical procedure, the NIST SRM3163 was prepared using our standard chemical separation procedure and treated as an unknown. The average $\epsilon W = -0.08 \pm 0.10$ (2σ, $n = 6$) for the chemically treated SRM3163 is plotted with dashed lines and the reproducibility is regarded as the minimum error for unknowns. In the case of the kimberlite data, the internal precision supersedes the reproducibility of the chemically treated SRM3163 and errors are therefore increased to ± 0.1 ϵW. Although the chemically treated SRM3163 is overlapping with the untreated standard SRM3163 solution, there is a systematic shift towards lower ϵW values.

We present W-isotope ratios for Hawaiian picrites and selected South African Group I and II kimberlites (Table 1). The Hawaiian samples are the same picrites for which a core-contribution has been invoked and so our results can be compared directly with the published Os isotope data[3,4]. Kimberlites were analysed as W isotope anomalies have been reported in these rocks and also attributed to core interactions[6]. The Hawaiian samples are tholeiitic picrites that erupted on the flanks of the Hawaiian volcanoes. In addition to Os isotopes, these samples have been analysed for a range of elements and isotope systems[16–18]. Kimberlite samples were selected from the major collection at the University of Cape Town to cover a range of Group I and Group II samples.

All measured ϵW values are within analytical error of our measurements of NIST SRM3163, the standard widely used as the silicate Earth reference (Fig. 1). Thus we find no obvious evidence for a core contribution in either the picrites or kimberlites.

We now explore two mixing models to investigate whether Os isotopic ratios might have been influenced by core addition with no significant effect on the W isotope ratios (Fig. 2). The ^{186}Os/^{188}Os ratio for the outer core is taken to be 0.119870 (ref. 3), and the key controlling factors in these models are then the terrestrial inventories of W and Os and their distribution between the outer and inner core, mantle and continental crust. The bulk Earth non-volatile element abundances are assumed to be 1.85 times C1 chondrite in both models[19], and it should be noted that lower estimates would straighten the mixing hyperbolae and so increase

Table 1 **W isotope data for samples and NIST SRM3163 standard solution**

Sample	Session	ϵ^{182}W	$\pm 2\sigma$	ϵ^{183}W	$\pm 2\sigma$
Kimberlites					
KK-6 kimberlite Gp I	2	−0.09	0.10	−0.06	0.08
K119/1 kimberlite Gp I	3	−0.05	0.10	−0.04	0.06
K119/2 kimberlite Gp I	3	−0.07	0.10	−0.03	0.04
NE-K6 kimberlite Gp II	3	−0.15	0.10	0.03	0.06
Hawaiian picrites					
LO-02-02	4	−0.16	0.21	−0.04	0.15
LO-02-02 repl 1	4	0.05	0.66	−0.16	0.36
LO-02-02 repl 2	4	0.05	0.37	0.06	0.26
LO-02-02 weighted average		−0.10	0.17	−0.03	0.12
LO-02-04	2	−0.14	0.21	0.07	0.17
H-11	1	−0.10	0.19	0.15	0.19
H-11 repl 1	1	−0.14	0.20	0.09	0.19
H-11 repl 2	1	−0.01	0.23	0.09	0.14
H-11 repl 3	2	−0.02	0.37	−0.08	0.27
H-11 weighted average		−0.08	0.11	0.08	0.09
CJH-02-05	1	0.01	0.35	0.05	0.19
CJH-02-05 repl 1	1	0.11	0.26	0.07	0.18
CJH-02-05 repl 2	1	−0.18	0.24	−0.10	0.19
CJH-02-05 weighted average		−0.04	0.16	0.01	0.10
Allende whole rock	5	−1.90	0.29	0.09	0.20
Replicate	5	−1.90	0.23	0.26	0.26
Coahuila IIAB iron	5	−3.49	0.10	−0.04	0.06
SRM after chemistry					
SRM 01	1	−0.20	0.18	−0.01	0.13
SRM 02	1	0.09	0.18	−0.01	0.14
SRM 03	4	−0.08	0.15	−0.09	0.09
SRM 05	4	−0.14	0.17	0.10	0.13
SRM 07	4	0.04	0.19	−0.08	0.13
SRM 08	4	−0.11	0.10	0.00	0.07
SRM weighted average		−0.08	0.10	−0.02	0.07
SRM standard solution		^{182}W/^{184}W	$\pm 2\sigma$	^{183}W/^{184}W	$\pm 2\sigma$
$n = 11$	1	0.864880	(3)	0.467115	(2)
$n = 13$	2	0.864812	(4)	0.467109	(4)
$n = 12$	3	0.864804	(6)	0.467122	(2)
$n = 17$	4	0.864775	(6)	0.467126	(1)
$n = 11$	5	0.864790	(7)	0.467137	(2)

ϵW data for South African Group I and Group II kimberlites and Hawaiian lavas relative to the weighted average for the untreated stock NIST SRM3163 standard solution for each analytical session. Amplifier gain calibration was made before all sessions except the first. Absolute ^{182}W/^{184}W and ^{183}W/^{184}W for NIST SRM3163 for each session are given at the bottom of the table and with 2σ errors for the last significant digit in brackets.

the expected effect on ϵW from core contribution (Fig. 2). W is siderophile during core formation and incompatible during mantle melting. Thus, the depleted mantle has low W abundances as a result of both of these processes. The W content of the core is calculated to 500 p.p.b. by mass balance using $W/Th_{sE} = 0.19$ and the reservoir masses of ref. 20. The concentration of W in the outer core, $[W]_{oc}$, is controlled by the amount of inner-core crystallization and partitioning between liquid and solid metal. We adopted the equations by Liu and Fleet[21] and assume 2 wt% sulphur in the bulk core and 5.5 wt% inner-core crystallization yields $[W]_{oc} = 490$ p.p.b. Increasing sulphur in the core will decrease the amount of W in the outer core. In the first model, the mantle has a W/Th ratio of 0.19 and $[W]_m = 8$ p.p.b., reflecting extraction of the continental crust from the whole mantle that has subsequently been homogenized by convection[22]. Enrichment of W in the continental crust is estimated by comparison with Th, assuming $[Th]_{cc} = 5{,}600$ p.p.b. and a $W/Th_{cc} = 0.20$, which yields 1,100 p.p.b. W (refs 12, 23). Brandon *et al.*[5] explore four different crystallization models for the inner core and we adopt the average $[Os]_{oc} = 300$ p.p.b. of their models three and four. The mantle end-member is assumed to have a $^{186}Os/^{188}Os = 0.1198345$ (ref. 3) and [Os] = 3.1 p.p.b. (ref. 9). The resulting mixing curve predicts $\epsilon W \approx -0.55$ for H-11, the most radiogenic Hawaiian picrite, if its elevated ^{186}Os is a result of the addition of core material. The weighted average ϵW for H-11 is clearly resolved from this mixing curve and there is therefore no support for core-derived Os using these first model parameters (Fig. 2).

As stated above, the core W isotope composition is fixed by mass balance and will not change through time. Although $^{186}Os/^{188}Os$ in the outer core and $[Os]_{oc}$ depend on the timing and extent of inner-core crystallization[5], we have assumed that $^{186}Os/^{188}Os$ in the outer core is 0.119870, following ref. 5. If we then wish to force a core-mantle mixing model through H-11, one way is to adopt model 1 of ref. 5, where inner-core crystallization was nearly complete by 4.3 Gyr ago. Early inner-core crystallization models allow a lower Pt/Os of the outer core and require a lower Os partition coefficient in the inner core, which implies a possible higher $[Os]_{oc} = 660$ p.p.b.: this higher $[Os]_{oc}$ will increase the mixing curvature. However, fast inner-core crystallization alone does not explain the data and a number of additional assumptions have to be made. (1) The minimum silicate Earth W-depletion to the core has to be such that Th/W = 0.26 and the W-extraction to the continental crust must all come from just the upper mantle, leaving the lower mantle with $[W]_{lm} = 19$ p.p.b.; (2) the core would need to contain 10 wt% sulphur, the maximum likely value; and (3) the bulk Earth composition must not have lower element abundances than our current estimate of 1.85 times C1 chondrite. Taken together these three conditions are needed to give a minimum $[W]_{oc} = 440$ p.p.b.. The resultant mixing curve (Fig. 2) is therefore tightly constrained to require fast inner-core crystallization, minimum W-depletion in silicate Earth and isolation of the lower mantle. Such an extreme model seems implausible and even so does not overlap the 2σ error of H-11.

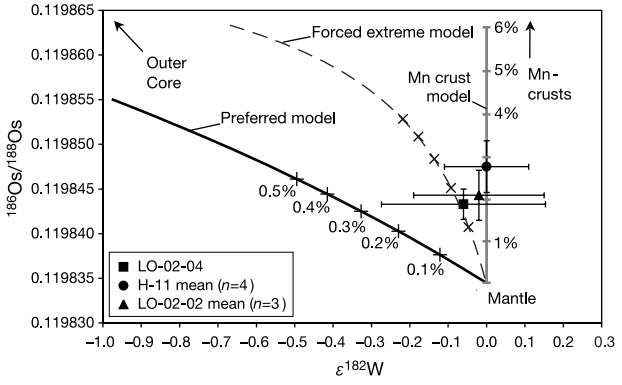

Figure 2 ϵW–$^{186}Os/^{188}Os$ mixing models for two core-contribution scenarios and for Mn-crust contamination of the Hawaiian plume source. (Os data from ref. 3.) Tick marks for the two core-contribution models represent 0.1 wt% core addition increments, whereas the tick marks for the Mn-crust model represent 1 wt% increments. Hawaiian picrites are plotted with 2σ error bars and were adjusted to the chemically treated SRM3163 by increasing their ϵW by 0.08 units to represent their relative composition more accurately. Even when errors are accounted for, the Hawaiian data are resolved from our preferred core-contribution model, although there is overlap for some of the data using more extreme parameters selected to maximize the chance of fitting. An alternative to the extreme core-contribution model is given by relatively small additions of Mn-crusts to the plume source. This model predicts no ϵW and readily fits the constraints from coupled ^{186}Os–^{187}Os trends in Hawaiian[1,2] and Gorgonan[3] lavas. Details of the mixing parameters are discussed in the text.

The lack of negative ϵW anomalies in kimberlites (Fig. 1) is at odds with previous data[6], where the most extreme anomalies are as low as some iron meteorites[24]. If correct, this would require the core to be considerably less radiogenic than the current estimate, and to balance the silicate Earth[13–15], a hidden highly radiogenic silicate reservoir. Our data require no core contribution in kimberlites, nor any additional hidden reservoir, but are nevertheless compatible with growing evidence for a strong subduction component in both whole-rock kimberlites and diamond inclusions[25,26].

If the core-contribution model is discarded, other means of obtaining the observed Os-anomalies has to be sought. The Os-data constrains any recycled component because few crustal sources have high enough Pt/Os ratios to develop suitable ^{186}Os enrichment. Mn-nodules have [Mn] ≈ 25%, high $^{190}Pt/^{188}Os \approx 0.2$–0.5 (ref. 27), low Re/Os ≈ 0.1–0.5 but high [Os] ≈ 1–3 p.p.b. and $^{187}Os/^{188}Os \approx 0.5$–1 (ref. 28). Using these values, ≤2–4% contamination from Mn-crusts to the peridotite source reproduces the Os isotope trends for Hawaii and Gorgona but predict no W-anomalies (Fig. 2). This model predicts a 5–9 times Mn-increase in the mantle source, and that Fe/Mn would decrease. Further detailed analyses are required to explore any correlations between Os-anomalies and Fe/Mn in the lavas, but major element compositions of erupted magmas are significantly influenced by conditions of melting, and modest variations in Mn and Fe of the source are not necessarily clearly evident in the composition of erupted melts. Brandon *et al.*[5] argued that the intersection point for the combined ^{186}Os–^{187}Os-trends from Gorgona, Hawaii and Siberia[29] may be interpreted as a single ubiquitous end-member, but we note that the range of Os compositions observed in Mn-nodules quite readily fit the uncertainty of the common intersection point reported[5] and this constraint may therefore not be a major problem for a recycling model. Moreover a recycled origin of ^{187}Os has been implicated in Hawaiian lavas using a combined study with $\delta^{18}O$ and it was suggested that heterogeneities on the length scale of only a few kilometres are preserved in the subducted slab[30]. If recycled Mn-crusts are confirmed to explain the ^{186}Os–^{187}Os data, further constraints for the length scales of preservation of subducted crust are obtained because Mn-crusts make up a volumetrically small component that veneers the surface of the subducted package. □

Methods

Hawaiian samples were prepared from fresh interiors of newly split hand specimens and care was taken to avoid any tools containing tungsten. Kimberlite powders were prepared from macrocryst-free matrix rocks and using tungsten-free equipment at the University of Cape Town. Samples were dissolved with equal amounts of concentrated HF and HNO_3 at 120 °C for 48–72 h in Savillex vials, except for chondrites that were dissolved at 180 °C with added $HClO_4$. Vials were pre-cleaned several times in HF and HNO_3 at 200 °C to leach out W (compare with ref. 14). Samples were dried down to dryness and treated with $HClO_4$ to break down fluorides. The sample was then dissolved in HCl and diluted to 1 M with added H_2O_2 or HF to complex W before being centrifuged and loaded on a pre-cleaned

Biorad AG-1 X8 100–200 mesh column of 2–4 ml, depending on sample size. Matrix elements were removed using ten column volumes (c.v.) of the loading acid and then conditioned with 0.5 c.v. HNO_3 + 0.5 M HF. W was eluted with 7 c.v. 4 M HNO_3 + 0.5 M HF and dried to dryness. Some samples were treated with equal parts H_2O_2 and 7 M HNO_3 to break down possible organic compounds. We note that several other protocols (for example, eluting in 8 M HCl + 1 M HF) gave poor yields and in some cases, caused artificial anomalies. Samples were analysed in static mode on either of the two Finnigan Neptune plasma ionization multi-collector mass spectrometers (PIMMS) at the University of Bristol. The samples were aspirated through either a Cetac Aridus desolvating nebulizer or an Apex HF nebulizer. The data were corrected for mass bias using $^{186}W/^{183}W = 1.98594$ and screened using the corrected $^{183}W/^{184}W$ for NIST SRM3163. Total analytical blank was 200–300 pg except for the Allende chondrites where a different batch of HF gave a considerably higher blank at 940 pg. The blank contribution was insignificant to all samples (>25 ng W) except the Allende chondrite (~60 ng). Three samples that deviated significantly from SRM3163 in its $^{183}W/^{184}W$ were rejected. All samples are reported in Table 1 relative to stock SRM3163 using the epsilon notation for both $^{182}W/^{184}W$ and $^{183}W/^{184}W$, and where SRM3163 ϵ ^{182}W and ϵ ^{183}W are both zero by definition.

Received 8 July; accepted 10 November 2003; doi:10.1038/nature02221.

1. Reisberg, L. *et al.* Os isotope systematics in ocean island basalts. *Earth Planet. Sci. Lett.* **120,** 149–167 (1993).
2. Hauri, E. H. & Hart, S. R. Re-Os isotope systematics of HIMU and EMII oceanic island basalts from the south-pacific ocean. *Earth Planet. Sci. Lett.* **114,** 353–371 (1993).
3. Brandon, A. D., Walker, R. J., Morgan, J. W., Norman, M. D. & Prichard, H. M. Coupled ^{186}Os and ^{187}Os evidence for core-mantle interaction. *Science* **280,** 1570–1573 (1998).
4. Brandon, A. D., Norman, M. D., Walker, R. J. & Morgan, J. W. ^{186}Os-^{187}Os systematics of Hawaiian picrites. *Earth Planet. Sci. Lett.* **174,** 24–42 (1999).
5. Brandon, A. D. *et al.* ^{186}Os-187Os systematics of Gorgona Island komatiites: implications for early growth of the inner core. *Earth Planet. Sci. Lett.* **206,** 411–426 (2003).
6. Collerson, K. D., Schoenberg, R. & Kamber, B. S. Unradiogenic W in kimberlites: direct evidence for core-mantle interaction. *Geochim. Cosmochim. Acta A* **66,** 148 (2002).
7. Hofmann, A. W. & White, W. M. Mantle plumes from ancient oceanic crust. *Earth Planet. Sci. Lett.* **57,** 421–436 (1982).
8. McKenzie, D. & O'Nions, R. K. Mantle reservoirs and ocean island basalts. *Nature* **301,** 229–231 (1983).
9. Shirey, S. B. & Walker, R. J. The Re-Os isotope system in cosmochemistry and high temperature geochemistry. *Annu. Rev. Earth Planet. Sci.* **26,** 423–500 (1998).
10. Shaefer, B. F., Turner, S., Parkinson, I., Rogers, N. & Hawkesworth, C. J. Evidence for recycled Archean oceanic mantle lithosphere in the Azores plume. *Nature* **420,** 304–307 (2002).
11. Walker, R. J., Morgan, J. W. & Horan, M. F. Osmium-187 enrichment in some plumes: evidence for core-mantle interaction? *Science* **269,** 819–822 (1995).
12. Newsom, H. E. *et al.* The depletion of tungsten in the bulk silicate Earth: constrainst on core formation. *Geochim. Cosmochim. Acta* **60,** 1155–1169 (1996).
13. Yin, Q. *et al.* A short timescale for terrestrial planet formation from Hf-W chronometry of meteorites. *Nature* **418,** 949–952 (2002).
14. Kleine, T., Münker, C., Mezger, K. & Palme, H. Rapid accretion and early core formation on asteroids and the terrestrial planets from Hf-W chronometry. *Nature* **418,** 952–955 (2002).
15. Schoenberg, R., Kamber, B., Collerson, K. D. & Eugster, O. New W-isotope evidence for rapid terrestrial accretion and very early core formation. *Geochim. Cosmochim. Acta* **66,** 3151–3160 (2002).
16. Norman, M. D. & Garcia, M. O. Primitive magmas and source characteristics of the Hawaiian plume: petrology and geochemistry of shield picrites. *Earth Planet. Sci. Lett.* **168,** 27–44 (1999).
17. Bennett, V. C., Esat, T. M. & Norman, M. D. Two mantle-plume components in Hawaiian picrites inferred from correlated Os-Pb isotopes. *Nature* **381,** 221–224 (1996).
18. Bennett, V. C., Norman, M. D. & Garcia, M. O. Rhenium and platinum group element abundances correlated with mantle source components in Hawaiian picrites: sulphides in the plume. *Earth Planet. Sci. Lett.* **183,** 513–526 (2000).
19. McDonough, W. F. in *Earthquake Thermodynamics and Phase Transformations in the Earth's Interior* Vol. 76 (eds Teisseyre, R. & Majewski, E.) 3–23 (Academic, San Diego, 2001).
20. Yoder, C. F. in *Global Earth Physics: a Handbook of Physical Constants* (ed. Ahrens, T. J.) 1–31 (American Geophysical Union, Washington DC, 1995).
21. Liu, M. & Fleet, M. E. Partitioning of siderophile elements (W, Mo, As, Ag, Ge, Ga, and Sn) and Si in the Fe-S system and their fractionation in iron meteorites. *Geochim. Cosmochim. Acta* **65,** 671–682 (2001).
22. Helffrich, G. R. & Wood, B. J. The Earth's mantle. *Nature* **412,** 501–507 (2001).
23. Rudnick, R. L. & Fountain, D. M. Nature and composition of the continental crust—a lower crustal perspective. *Rev. Geophys.* **33,** 267–309 (1995).
24. Horan, M. F., Smoliar, M. I. & Walker, R. J. ^{182}W and ^{187}Re-^{187}Os systematics of iron meteorites: Chronology for melting, differentiation, and crystallization in asteroids. *Geochim. Cosmochim. Acta* **62,** 545–554 (1998).
25. Smith, C. B. Pb, Sr and Nd isotopic evidence for sources of southern African cretaceous kimberlites. *Nature* **304,** 51–54 (1983).
26. Schulze, D. J. *et al.* Extreme crustal oxygen isotope isotope signature preserved in coesite in diamond. *Nature* **423,** 68–70 (2003).
27. Peucker-Ehrenbrink, B. & Ravizza, G. The marine osmium isotope record. *Terra Nova* **12,** 205–219 (2000).
28. Burton, K. W. *et al.* Osmium isotope variations in the oceans recorded by Fe–Mn crusts. *Earth Planet. Sci. Lett.* **171,** 185–197 (1999).
29. Walker, R. J. *et al.* Applications of the ^{190}Pt-^{186}Os isotope system to geochemistry and cosmochemistry. *Geochim. Cosmochim. Acta* **61,** 4799–4807 (1997).
30. Lassiter, J. C. & Hauri, E. H. Osmium-isotope variation in Hawaiian lavas: evidence for recycled oceanic lithosphere in the Hawaiian plume. *Earth Planet. Sci. Lett.* **164,** 483–493 (1998).

Acknowledgements We thank A. LeRoex, J. Gurney, K. Westerlund, N. Coe and M. Coetzee at the University of Cape Town who provided and helped us select kimberlite samples. S. Russel at the Natural History Museum, London, donated the meteorite samples. Discussions on the manuscript by E. Hauri, G. Helffrich & B. Wood are appreciated. This work is supported by a EU Marie Curie post-doctoral fellowship.

Competing interests statement The authors declare that they have no competing financial interests.

Correspondence and requests for materials should be addressed to A.S. (anders.schersten@bristol.ac.uk).

Fossil embryos from the Middle and Late Cambrian period of Hunan, south China

Xi-ping Dong[1], Philip C. J. Donoghue[2], Hong Cheng[3] & Jian-bo Liu[1]

[1]*Department of Geology, Peking University, Beijing 100871, People's Republic of China*
[2]*Department of Earth Sciences, University of Bristol, Wills Memorial Building, Queens Road, Bristol BS8 1RJ, UK*
[3]*College of Life Sciences, Peking University, Beijing 100871, People's Republic of China*

Comparative embryology is integral to uncovering the pattern and process of metazoan phylogeny[1], but it relies on the assumption that life histories of living taxa are representative of their antecedents. Fossil embryos provide a crucial test of this assumption and, potentially, insight into the evolution of development, but because discoveries so far[2–5] lack phylogenetic constraint, their significance is moot. Here we describe a collection of embryos from the Middle and Late Cambrian period (500 million years ago) of Hunan, south China, that preserves stages of development from cleavage to the pre-hatching embryo of a direct-developing animal comparable to living Scalidophora (phyla Priapulida, Kinorhyncha, Loricifera). The latest-stage embryos show affinity to the Lower Cambrian embryo *Markuelia*[3], whose life-history strategy contrasts both with the primitive condition inferred for metazoan phyla and with many proposed hypotheses of affinity[3,6], all of which prescribe indirect development. Phylogenetic tests based on these embryological data suggest a stem Scalidophora affinity. These discoveries corroborate, rather than contradict, the predictions of comparative embryology, providing direct historical support for the view that the life-history strategies of living taxa are representative of their stem lineages.

All of the embryos are preserved in calcium phosphate with varying degrees of fidelity, from extremes in which structures of less than 0.3 μm are preserved, to others in which it is possible to make out only the general outline of the embryos; most specimens show a microspheritic surface texture indicative of bacterially mediated soft-tissue replacement[7].

The embryos vary in size and in the developmental stages represented. The smallest (diameter 236 μm) and earliest (Fig. 1a, b) stage is a cleavage embryo preserving the surface boundaries between blastomeres. Although not complete, dividing the surface area of the embryos by the average cell area suggests 485 cells. The remaining collection of embryos (for example, Fig. 1c–f) range in diameter from 370 to 411 μm. Three further specimens (for example, Fig. 1c) are later developmental stages but do not fully occupy the volume of the embryo, and much of the surface area preserves undifferentiated tissue, probably yolk.